ELSEVIER

Journal of Alloys and Compounds 320 (2001) 234–241

Journal of ALLOYS AND COMPOUNDS

www.elsevier.com/locate/jallcom

Thermodynamic calculation of the In–Sn–Zn ternary system

Y. Cui*, X.J. Liu, I. Ohnuma, R. Kainuma, H. Ohtani, K. Ishida

Department of Materials Science, Graduate School of Engineering, Tohoku University, Aoba-yama 02, Sendai 980-8579, Japan

---

Abstract

A thermodynamic description of the In–Sn–Zn ternary system, which is of technical importance to optimize lead-free solder alloys, is presented using the CALPHAD method. Phase equilibria, such as isothermal and vertical sections, liquidus projection and mole fractions of the phase constitution, and thermochemical quantities were calculated and compared with the experimental data. They are in excellent agreement in most cases. © 2001 Elsevier Science B.V. All rights reserved.

Keywords: Thermodynamic calculation; Phase diagram; Indium; Tin; Zinc; Solder

---

1. Introduction

Over several years, much effort was put into developing alternative lead-free solder alloys due to the environmental and health concerns on lead usage. Among many potential substitutes, Sn–Zn-based alloys were viewed as very promising candidates [1]. Recently, MacCormack et al. [2] demonstrated that the addition of In into the Sn–Zn alloys can positively contribute to the wetting characteristics of the alloys and lower sufficiently their melting temperatures. Furthermore, a solder alloy, Sn 86%, In 5%, Zn 9% (wt.), with sufficient similar melting points to the eutectic Pb–Sn solders, was developed and proved experimentally as a drop-in replacement for the traditional Pb–Sn solders. Accordingly, an appropriate thermodynamic description of the In–Sn–Zn ternary system is desirable to design and optimize the composition and microstructure of the alloys.

Many investigations contributed to the determination of both phase relation and thermodynamic properties of the In–Sn–Zn system. Spengler [3] reported his pioneering study in 1954, where an entire, but primary, liquidus projection was constructed. Recently, MacCormack and Jin [1,2] studied the melting behavior of two ternary alloys, Sn 86%, In 5%, Zn 9% and Sn 81%, In 10%, Zn 9% (wt.), and reported their melting points were 188 and 178°C, respectively. More recently, Yoon et al. [4] analyzed several specific ternary alloys by differential scanning calorimetry (DSC) measurement, supplemented by scanning electron microscopy (SEM) and X-ray diffractometry (XRD). Two partial vertical sections and the liquidus projection were subsequently constructed combining a primary thermodynamic calculation and the experimental results. Later on, in a DTA lattice parameter and micro-probe measurement on 40 ternary alloys, Xie et al. [5] constructed three cross sections with constant Sn to Zn ratio of 2:1, 1:1 and 1:2, as well as one with 10 at.% In.

Moser [6] determined the thermodynamic properties of dilute liquid zinc solutions of the In–Sn–Zn system by means of the emf method at 714, 757 and 805 K, respectively. Most recently, performing on a Calvet type drop calorimeter, Fiorani et al. [7] investigated the enthalpy of mixing of the In–Sn–Zn liquid homogeneous phase following three isopletic cuts, i.e. In:Sn=In:Zn=Sn:Zn=1:1, as a border ternary system of the In–Pb–Sn–Zn quaternary system.

The aim of this work is to critically evaluate the previous works and develop a set of parameters of the In–Sn–Zn ternary system using the CALPHAD method, which is one of our serial studies on the thermodynamic database for the micro-soldering alloys including the elements of Pb, Bi, Sn, Sb, Cu, Ag, Zn and In [8,9].

2. Evaluation of previous works

2.1. Experimental data of the ternary system

As regards the exploring work by Spengler [3], only the accessible experimental points on the ternary eutectic reaction, rather than the graphical liquidus surface, were adopted in this work. Although the number of alloys analyzed by Ref. [2] was too few to determine any phase

---

*Corresponding author.

0925-8388/01/$ – see front matter
PII: S0925-8388(00)01484-5

boundaries accurately, the conclusion extracted from their experiment can also serve as a guideline during the assessment, i.e. the introduction of In in the Sn–Zn alloys can effectively lower their melting points.

Yoon et al. [4] reported two partial cross sections with 9 and 6 wt.% Zn. These two sections are critical to evaluate and optimize the In–Sn–Zn solders in service. The following section will recalculate them and make a comparison between them with their respective former versions.

The study by Xie et al. [5] was visualized as the most extensive and elaborate work on this system up to now. All their data were thus accepted in this work. However, it should be noted that the deviation between the heating and cooling liquidus curves at a low zinc content is obvious. Xie et al. already pointed out that, at a low zinc content, the peaks of the heating curves corresponding to the liquidus temperatures were very flat and it was difficult to determine the accurate liquidus temperatures. It could be therefore expected that those heating data may involve large system errors and hence were attached a low weight during optimization. Concerning the probable serious contamination and undercooling of liquid in the cooling measurement, which are usually experienced in the low melting temperature solders research, all the cooling data were also given a relative low weight.

Moser [6] determined the activities of Zn in the dilute alloys solution at 3, 5, 7 and 10 at.% Zn. But all the experimental values were just marked in small charts rather than the favored tabulation lists, with the exception of 3 at.% Zn. As a result, only the data at 3 at.% Zn were taken into account in this work, although his data were generally regarded as quite reliable. The enthalpies of mixing of the liquid phase due to Fiorani et al. [7] were also employed to adjust the parameters of the liquid phase.

2.2. *Assessment of the binary systems*

Lee et al. [10,11] have assessed three binary systems, In–Sn, In–Zn and Sn–Zn, in their serial works on lead-free solder alloys. Afterwards, Korhonen and Kivilahti [12] independently developed another set of parameters of the In–Sn binary system including the related metastable lattice stabilities. The earlier version [10] on the In–Sn system was adopted to ensure the continuity and feasibility of our multicomponent lead-free solder alloy database, as well as its extrapolation ability. The In–Zn was also extracted from Lee's results [11]. Since Ohtani et al. [13] recently reassessed the Sn–Zn system, in which a different lattice stability of hcp-Sn was employed, this updated result was used in this work.

3. Thermodynamic model and optimization procedure

The substitutional solution model was used to describe

Table 1
Summary of the parameters assessed in the present work and the binary parameters from the selected literature (values for solution phases are given in J/mol of atoms)

System	Phase	Parameters	Ref.
In–Sn	Liquid	${}^{0}L^{\text{liquid}}_{\text{In,Sn}} = -711 - 1.6934 \times T$	[10]
		${}^{1}L^{\text{liquid}}_{\text{In,Sn}} = -64 - 1.3592 \times T$	
	Bct-(Sn)	${}^{0}L^{\text{bct-(Sn)}}_{\text{In,Sn}} = -239 + 2.8509 \times T$	[10]
	Tet-(In)	${}^{0}L^{\text{tet-(In)}}_{\text{In,Sn}} = +743 - 3.3139 \times T$	[10]
		${}^{1}L^{\text{tet-(In)}}_{\text{In,Sn}} = -1487$	
	γ	${}^{0}G^{\gamma}_{\text{In}} = +\text{GHSERIN} + 10\,292.5 - 7.64 \times T$	
		${}^{0}G^{\gamma}_{\text{Sn}} = +\text{GHSERSN} + 925.3 - 1.7562 \times T$	[10]
		${}^{0}L^{\gamma}_{\text{In,Sn}} = -15\,715.5 + 19.3402 \times T$	
	β	${}^{0}G^{\beta}_{\text{In}} = +\text{GHSERIN}$	
		${}^{0}G^{\beta}_{\text{Sn}} = +\text{GHSERSN} + 5015.5 - 7.5 \times T$	[10]
		${}^{0}L^{\beta}_{\text{In,Sn}} = -235 - 3.6954 \times T$	
In–Zn	Liquid	${}^{0}L^{\text{liquid}}_{\text{In,Zn}} = +12\,401 - 4.4498 \times T$	
		${}^{1}L^{\text{liquid}}_{\text{In,Zn}} = -3186 + 1.756 \times T$	[11]
		${}^{2}L^{\text{liquid}}_{\text{In,Zn}} = 679$	
	Tet-(In)	${}^{0}L^{\text{tet-(In)}}_{\text{In,Zn}} = +4430 - 4.4498 \times T$	[11]
		${}^{1}L^{\text{tet-(In)}}_{\text{In,Zn}} = 9717$	
	Hcp-(Zn)	${}^{0}L^{\text{hcp-(Zn)}}_{\text{In,Zn}} = 23\,114$	[11]
Sn–Zn	Liquid	${}^{0}L^{\text{liquid}}_{\text{Sn,Zn}} = +12\,710 - 9.162 \times T$	
		${}^{1}L^{\text{liquid}}_{\text{Sn,Zn}} = -5360 + 3.45 \times T$	[13]
		${}^{2}L^{\text{liquid}}_{\text{Sn,Zn}} = 835$	
	Bct-(Sn)	${}^{0}L^{\text{bct-(Sn)}}_{\text{Sn,Zn}} = 9260$	[13]
	Tet-(Sn,Zn)	${}^{0}L^{\text{tet-(Sn,Zn)}}_{\text{Sn,Zn}} = 8000$	This work
	Hcp-(Zn)	${}^{0}G^{\text{hcp-(Zn)}}_{\text{Sn}} = \text{GHSERSN} + 2400 - 3.1 \times \text{T}$	[13]
		${}^{0}G^{\text{hcp-(Zn)}}_{\text{Sn,Zn}} = 40\,000$	
In–Sn–Zn	Liquid	${}^{0}L^{\text{liquid}}_{\text{In,Sn,Zn}} = -2001 - 3.61 \times T$	
		${}^{1}L^{\text{liquid}}_{\text{In,Sn,Zn}} = 832 - 4.2 \times T$	This work
		${}^{2}L^{\text{liquid}}_{\text{In,Sn,Zn}} = -16\,257 + 21.2 \times T$	

all the phases in the system. The model yields the following expression for the Gibbs energy:

$$G_m = x_{\mathrm{In}}{}^{\circ}G_{\mathrm{In}} + x_{\mathrm{Sn}}{}^{\circ}G_{\mathrm{Sn}} + x_{\mathrm{Zn}}{}^{\circ}G_{\mathrm{Zn}} + RT(x_{\mathrm{In}}\ln x_{\mathrm{In}} + x_{\mathrm{Sn}}\ln x_{\mathrm{Sn}} + x_{\mathrm{Zn}}\ln x_{\mathrm{Zn}}) + {}^{\mathrm{ex}}G_m. \quad (1)$$

The parameter ${}^{\circ}G_i$ is the Gibbs energy of pure component i which was taken from the database [14] or the accepted binary systems. The excess energy ${}^{\mathrm{ex}}G_m$ can be derived from the binary excess Gibbs energy ${}^{\mathrm{ex}}G_{i,j}$ (i, $j=$In, Sn and Zn) using the Muggianu extrapolation model [15]:

$${}^{\mathrm{ex}}G_m = \sum_{i=1}^{2}\sum_{j=i+1}^{3}[x_i x_j/(V_{i,j}\cdot V_{j,i})]\cdot {}^{\mathrm{ex}}G_{i,j} + x_{\mathrm{In}}x_{\mathrm{Sn}}x_{\mathrm{Zn}}(x_{\mathrm{In}}L_{\mathrm{In}} + x_{\mathrm{Sn}}L_{\mathrm{Sn}} + x_{\mathrm{Zn}}L_{\mathrm{Zn}}). \quad (2)$$

L_i denotes ternary interaction parameter, the terms $V_{i,j}$ and $V_{j,i}$ are represented by:

$$V_{i,j} = \frac{1 + x_i - x_j}{2} \text{ and } V_{j,i} = \frac{1 + x_j - x_i}{2}. \quad (3)$$

The optimization of parameters was carried out using the Parrot module in the Thermo-Calc program developed by Sundman et al. [16]. At first, two sets of the experimental thermodynamic data [6,7] were taken into account to simultaneously optimize the ternary interaction parameters of liquid. The interaction parameters of various solid phases were then optimized by fitting the phase diagram data. It is to emphasize that, no ternary compound parameters were introduced to β and γ with lack of the confirmed ternary homogeneity ranges. It was also found, during the optimization, only a metastable binary regular parameter, ${}^{0}L^{\mathrm{tet}}_{\mathrm{Sn,Zn}}$, is inevitably required to satisfactorily reproduce most of the experimental data. As a result, only four parameters were employed in this work, i.e. three for liquid and one for tetragonal.

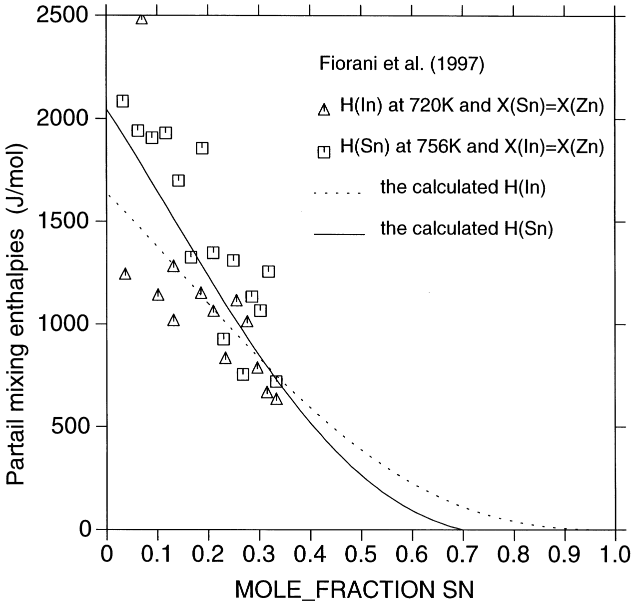

Fig. 2. Calculated partial mixing enthalpies of In and Sn in liquid at 720 and 756 K, following the isopletic cuts Sn:Zn=1:1 and In:Zn=1:1, respectively.

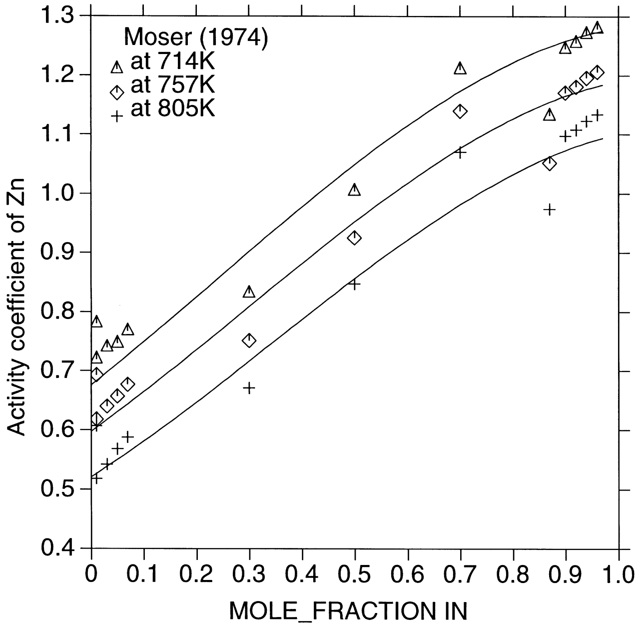

Fig. 1. Calculated activity coefficient of Zn in the liquid phase with 3 at.% Zn at 714, 757 and 805 K, respectively, compared with the experimental data.

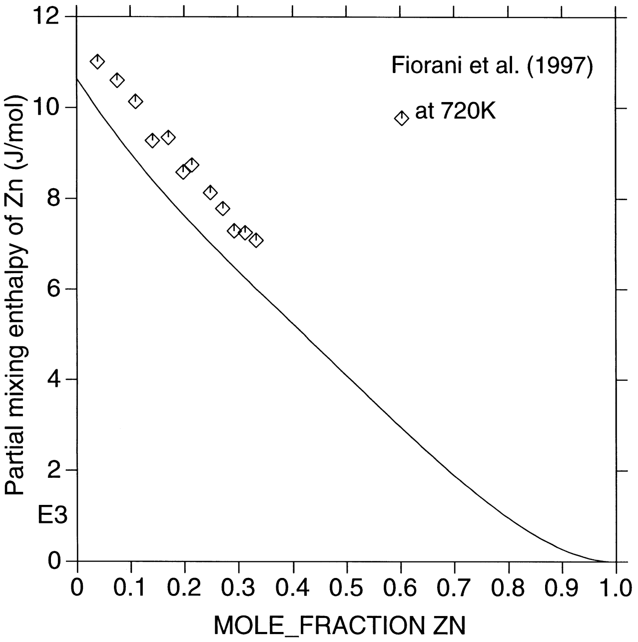

Fig. 3. The comparison between the calculated partial mixing enthalpy of Zn in liquid with In:Sn=1:1 at 720 K and the experimental data.

4. Results and discussion

The parameters assessed in this work are summarized in Table 1, as well as the accepted binary parameters of the In–Sn [10], In–Zn [11] and Sn–Zn system [13].

Fig. 1 illustrates the comparison between the calculated activity coefficient of Zn in liquid and the experimental data [6] at 714, 757 and 805 K with 3 at.% Zn. It is obvious that the agreement is very satisfactory with reference to the experimental data of a certain scatter in the middle In contents. The calculation does not compare so nicely with the data from Ref. [7], but for the fact all are indeed within the claimed experimental uncertainty, as presented in Figs. 2 and 3.

Fig. 4a–c show excellent agreements between the calculated vertical sections and the experimental data at

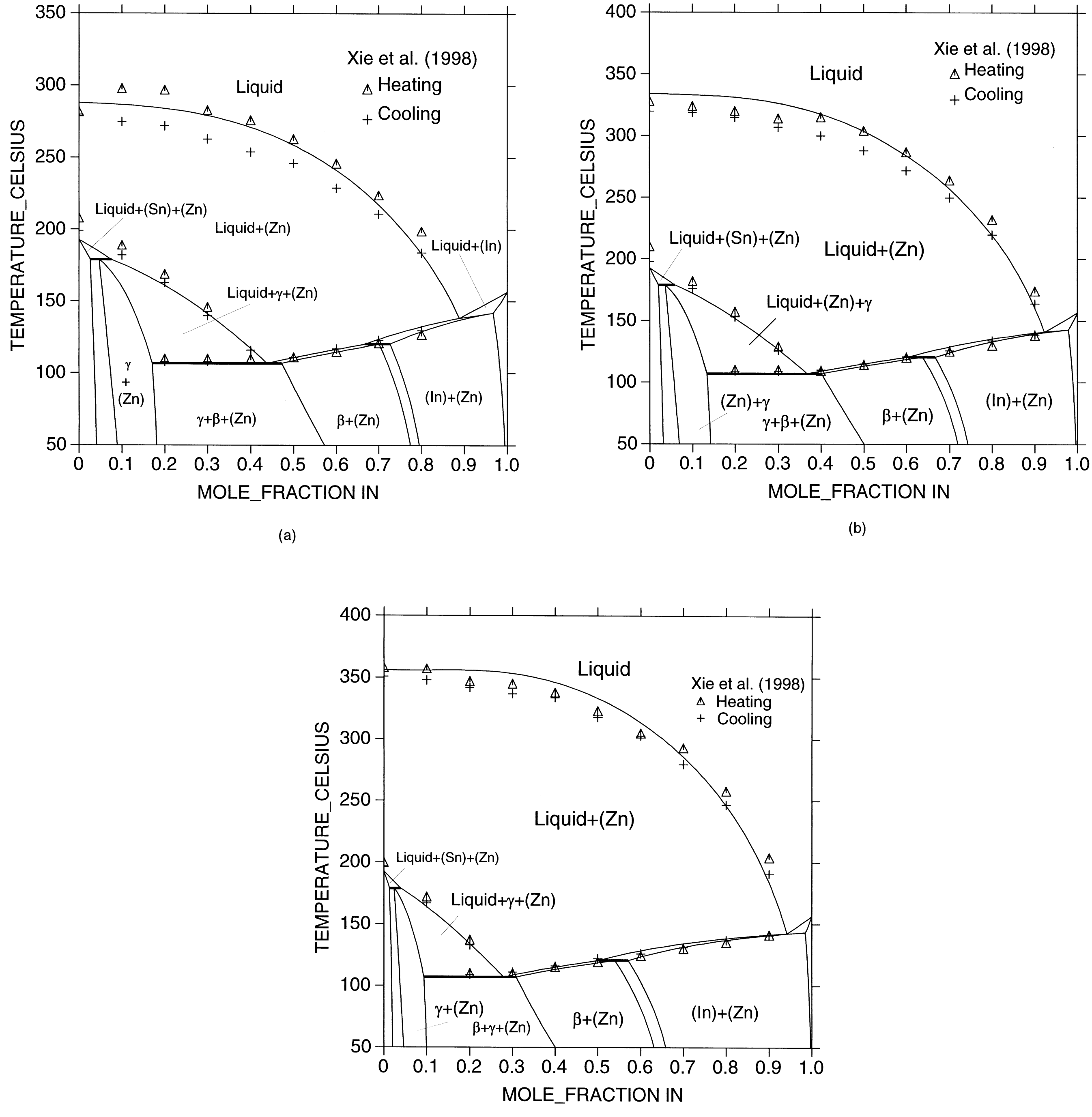

Fig. 4. Calculated vertical sections of the In–Sn–Zn ternary system at: (a) Sn:Zn = 2:1; (b) Sn:Zn = 1:1; and (c) Sn:Zn = 1:2 in comparison with the experimental data.

Sn:Zn = 2:1, 1:1 and 1:2, respectively. As already explained in Section 2, no further attempt was made to better fit the heating data at the low zinc content, as well as all the cooling data. Fig. 5 gives a full computed representation of the determined vertical sections with the constant 10 at.% In [5]. Although the present results cannot also replicate two single γ phase alloys (Sn 80%, In 10%, Zn 10% and Sn 65%, In 10%, Zn 25% (at.)) well, however, they could derive a more reasonable phase relation compared with those by Xie et al. A γ + [Sn] + [Zn] three-phase region was newly confirmed to locate at the low temperature; such a phase distribution is fully in accord with the binary information. The deficient section by Xie et al. is clearly due to an overlook of the [In] + γ two-phase region.

Fig. 6a and b represent the calculated vertical sections with the constant 9 and 6 wt.% Zn, respectively. As shown in the figures, the calculated liquidus exhibits a large discrepancy with the experimental values. A similar reason as for the heating data from Xie et al. should be expected to hold for this case. The present work also supported that the Sn 81%, In 10%, Zn 9% (wt.) alloy falls within the [Zn] + γ two-phase field at 160°C confirmed by the XRD measurement [4]. Additionally, to give a full representation of phase relation, Fig. 7a and b show two predicted isothermal sections of the In–Sn–Zn system at 100°C and 200°C, respectively. These two figures undoubtedly suggest, together with Fig. 6a and b, the optimum indium concentration for an In–Sn–Zn base solder is around 2–5 wt.%, since a favored simple microstructure without the γ phase, in essence, is achievable.

The calculated liquidus projection of the In–Sn–Zn ternary system is presented in Fig. 8a. Fig. 8b provides detailed information at the Sn-rich corner, which clearly indicates the zinc-rich side of the eutectic should be avoided because the liquidus temperature increases significantly with increasing zinc concentration. Table 2 lists the calculated invariant reactions including observed ternary invariant equilibria. It can be seen from it that the ternary eutectic reaction (E) is calculated to occur at the composition of Sn 46.2%, In 52.2%, Zn 1.6% (wt.) at 107°C, which compares well to the experimentally reported Sn 46.0%, In 52.2%, Zn 1.8% (wt.) at 108°C [3]. It is interesting to find that the invariant temperature of U1 is

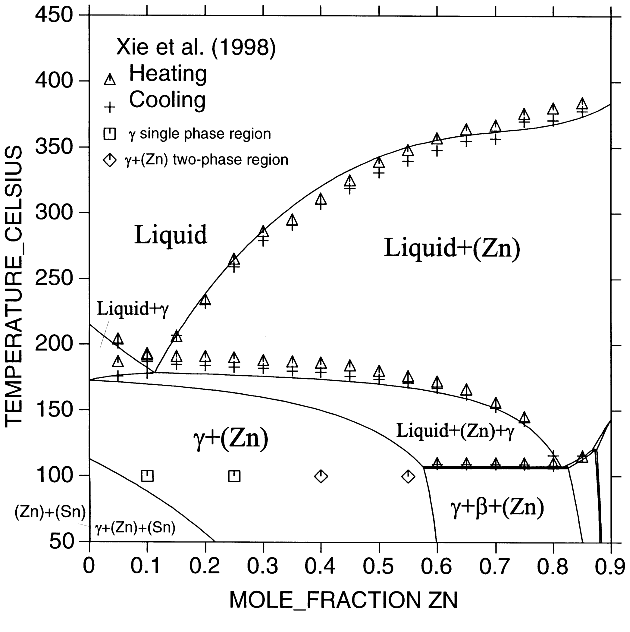

Fig. 5. Calculated vertical section of the In–Sn–Zn ternary system at 10 at.% In in comparison with the experimental data.

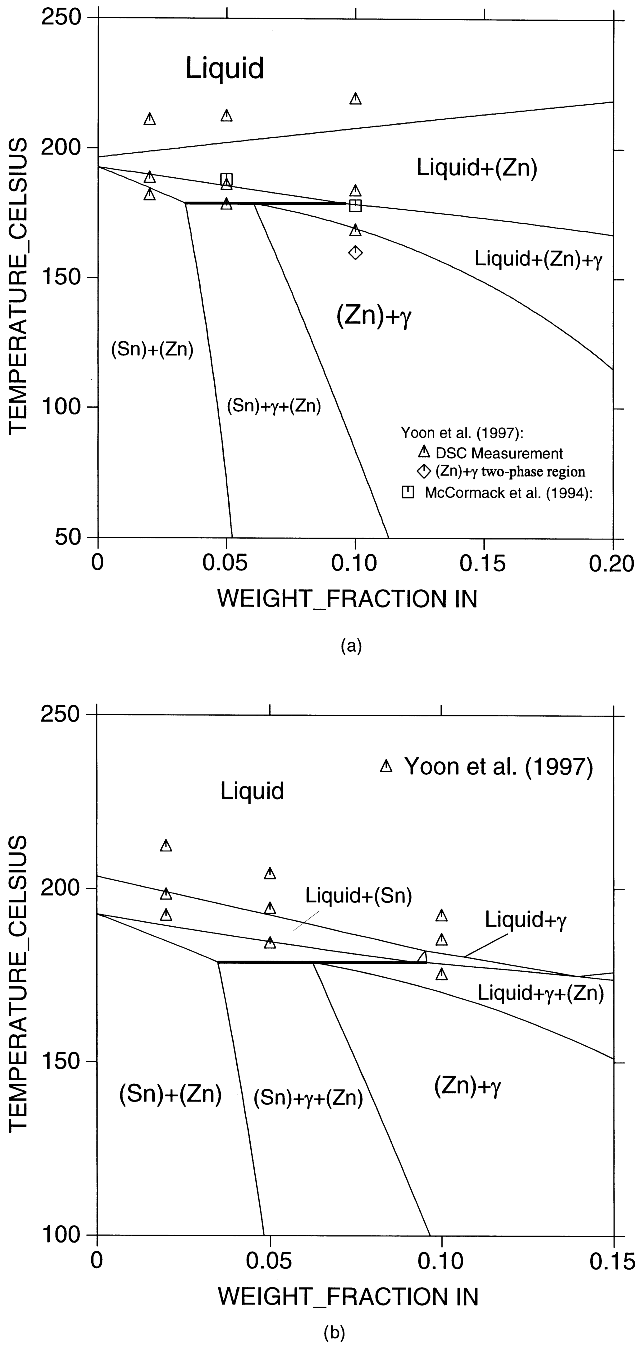

Fig. 6. Calculated vertical sections of the In–Sn–Zn ternary system at: (a) 9 wt.% Zn; (b) 6 wt.% Zn in comparison with the experimental data.

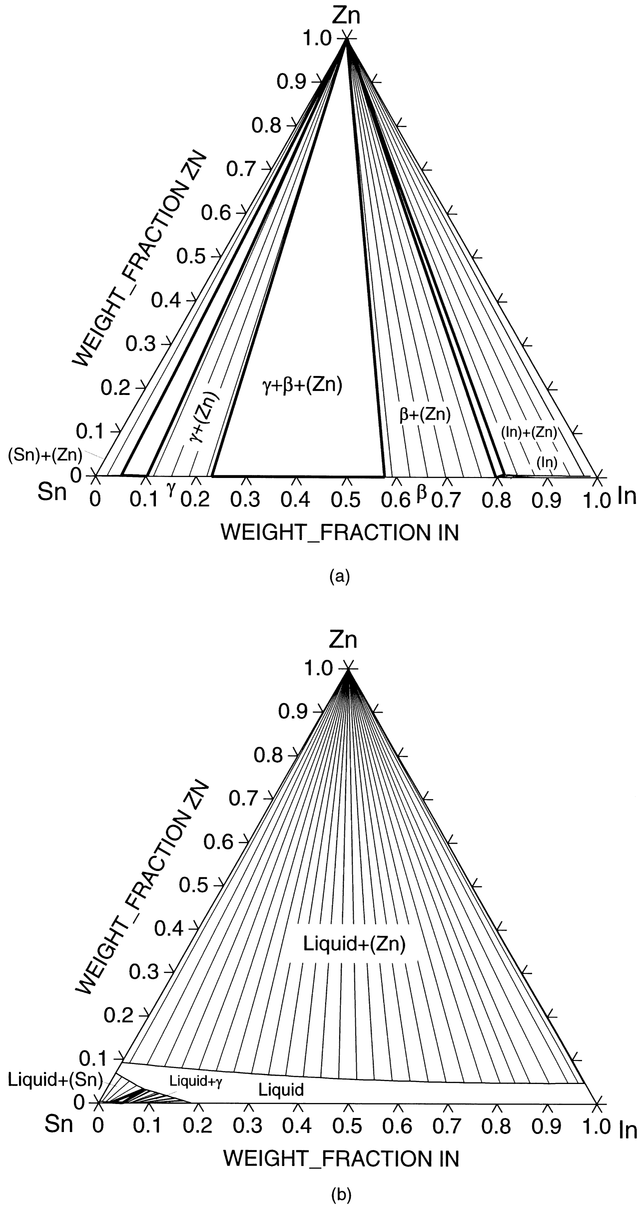

Fig. 7. Calculated isothermal section of the In–Sn–Zn ternary system at: (a) 100°C and (b) 200°C.

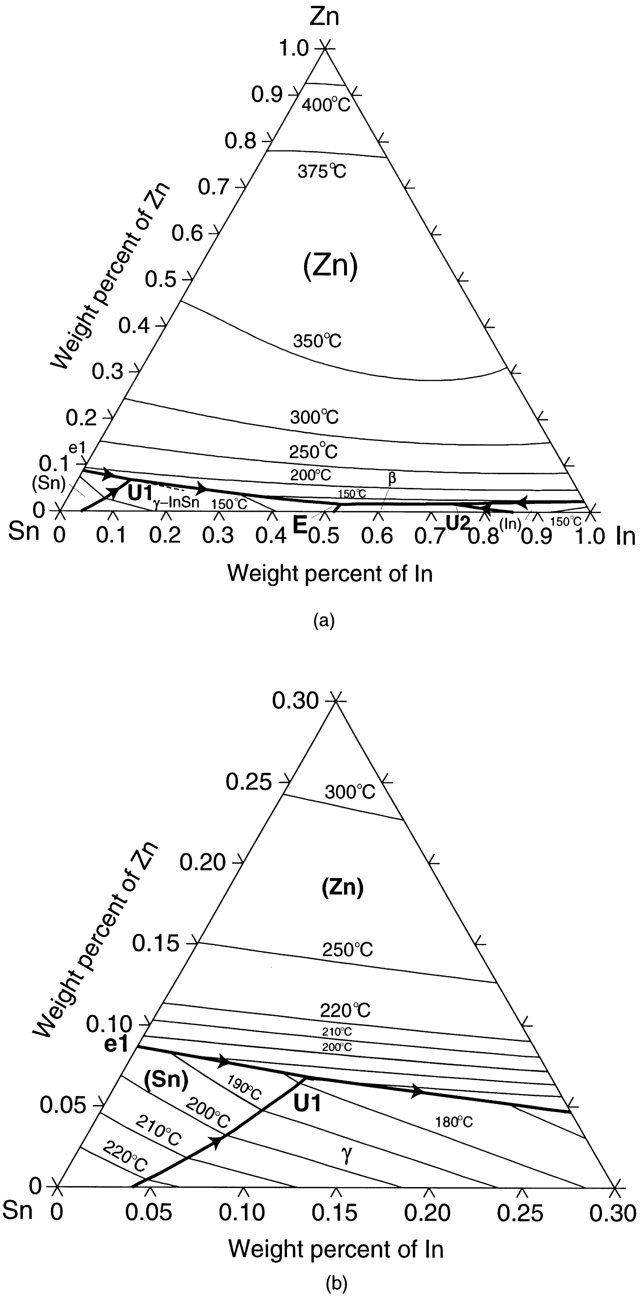

Fig. 8. (a) The entire calculated liquidus projection of the In–Sn–Zn ternary system; (b) an enlarged portion at the Sn-rich corner.

Table 2
Comparison of the calculated invariant reactions with the literature data

Reaction	Type	Temperature (°C)	Composition of the liquid phase (wt.%)			Ref.
			In	Sn	Zn	
L⇔[Zn]+γ+β	E	108	52.2	46.0	1.8	Exp., [3]
		107	52.2	46.2	1.6	Cal., this work
		109				Exp., [5]
		105	52.2	45.8	2.0	Cal., [4]
L+[In]⇔[Zn]+β	U2	120	73.2	25.1	1.7	Cal., this work
L+[Sn]⇔[Zn]+γ	U1	178	9.9	83.5	6.6	Cal., this work

very close to the Pb–Sn eutectic temperature. As a consequence, in Fig. 9a, the phase fractions of alloy U1 during cooling were calculated following the Level rule. Obviously, it indicates that this alloy is far from a suitable solder even though it has a favored melting temperature, because it would contain the undesirable soft compound γ of a large phase fraction in case of attainment of equilibrium in service. In a more detailed inspiration, Scheil calculation was carried out for this alloy, as shown in Fig. 9b. In comparison to the Level rule, this model describes another limiting case; it assumes that no back diffusion occurs in the solid state and perfect mixing in the liquid phase. For most alloys, however, Scheil calculation can still provide a prediction close to reality. It is noted that the formation of ternary eutectic due to segregation in the Scheil model solidification drastically increases the freezing range. Quite the contrary, a critical practical requirement for solders is a limited freezing range.

To investigate the effect of added In on the Sn–Zn eutectic alloys in more depth, the e1–U1 cross section was calculated in Fig. 10. It is obvious that the binary Sn–Zn eutectic reaction is suitably depressed with the increase of In until the ternary peritectic reaction U1 is reached. Comparing with the vertical section at 9 wt.% Zn in Fig. 6a, a very similar phase relation can be found in Fig. 10. It should be emphasized that, however, their respective effects of added In on the liquidus temperature and the freezing range are remarkably different; the incorporation of In increases the liquidus temperature and the temperature range of two- or three-phase field including liquid at 9 wt.% Zn, while decreaseing both features in the cross section of e1–U1. These facts suggest that the alloys within the range of 2–5 wt.% located at the e1–U1 line, characterized by their similar melting behavior to that of Sn–Pb eutectic alloys, are more suitable for the lead-free solders rather than the Sn 89–86%, Zn 9%, In 2–5% (wt.) alloys. These findings are different to the conclusion in Fig. 8b, but equally satisfactory in results, which are important for use in the design of new solder alloys.

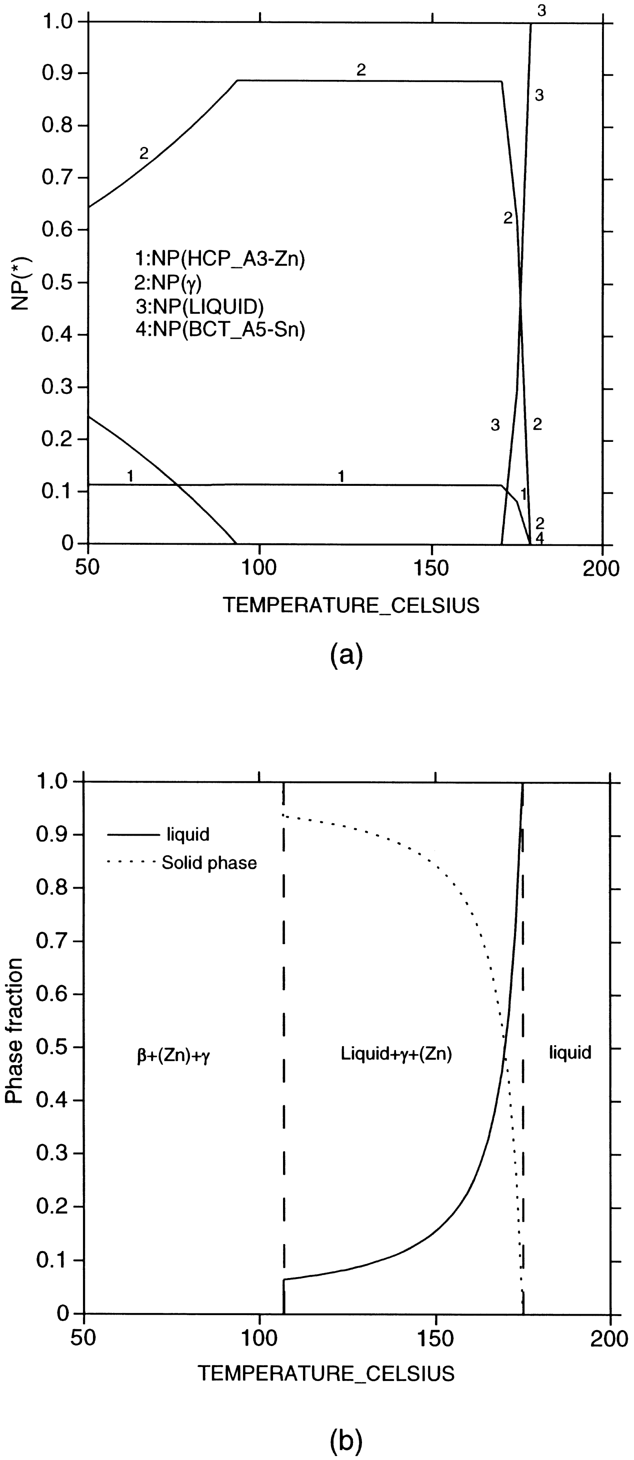

Fig. 9. Calculated phase fractions of alloy U1 during cooling following: (a) the Level rule and (b) Scheil calculation.

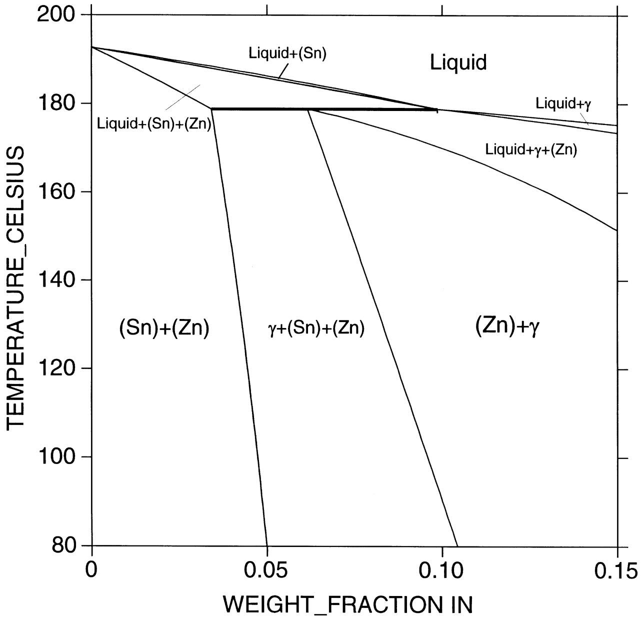

Fig. 10. Calculated e1–U1 cross section of the In–Sn–Zn ternary system.

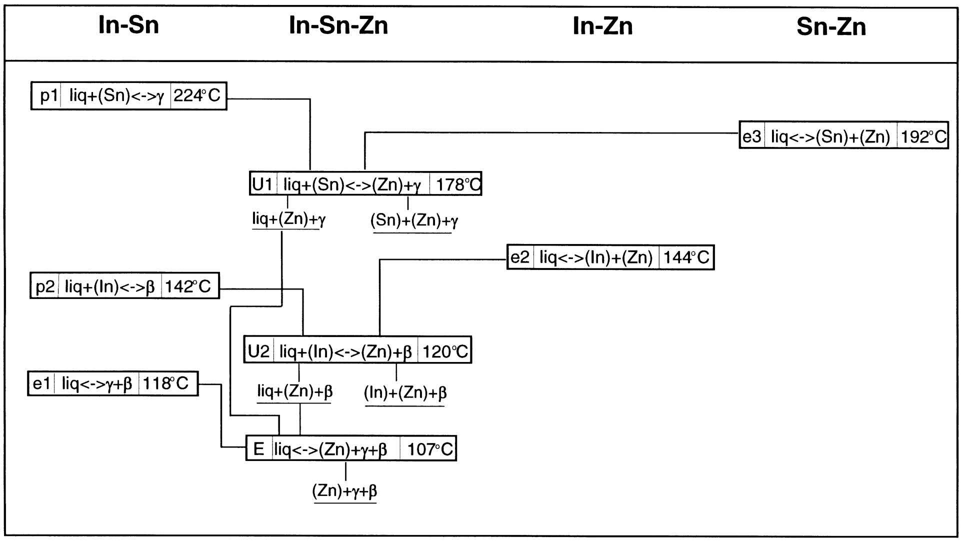

Fig. 11. The reaction scheme of the In–Sn–Zn ternary system.

For a fuller understanding of the phase relation, the reaction scheme is given in Fig. 11.

5. Conclusion

A thermodynamic description of the In–Sn–Zn ternary system was developed using the CALPHAD method in this work. A number of thermochemical quantities and vertical sections were calculated and compared with the experimental data. These are in excellent agreement in most cases. The present calculation can serve as a basic knowledge to design and optimize Sn–Zn-based solder alloys and also a border ternary system of the multicomponent solder systems.

References

[1] M. McCormack, S. Jin, J. Electron. Mater. 23 (1994) 687.
[2] M. McCormack, S. Jin, J. Electron. Mater. 23 (1994) 635.
[3] H. Spengler, Metall, Berlin 8 (1954) 936.
[4] S.W. Yoon, J.R. Soh, B.J. Lee, H.M. Lee, in: R.K. Mahidhara, D.R. Frear, S.M.L. Saty, K.L. Murty, P.K. Liaw, W. Winterbottom (Eds.), Design and reliability of solders and solders interconnections, The Mineral, Metals and Materials Society, 1997, p. 121.
[5] Y. Xie, H. Schicketanz, A. Mikura, Ber. Bunssenges. Phys. Chem. 102 (1998) 1334.
[6] Z. Moser, Z. Metallkde. 65 (1974) 106.
[7] J.M. Fiorani, C. Naguet, J. Hertz, A. Bourkba, L. Bouirden, Z. Metallkde. 88 (1997) 711.
[8] I. Ohnuma, X.J. Liu, H. Ohtani, K. Ishida, J. Electron. Mater. 28 (1999) 1163.
[9] I. Ohnuma, X.J. Liu, H. Ohtani, K. Ishida, in: K. Grassie et al. (Eds.), Functional Materials, Euromat-99, Vol. 13, 2000, p. 69.
[10] B.J. Lee, C.S. Oh, J.S. Shim, J. Electron. Mater. 25 (1996) 983.
[11] B.J. Lee, CALPHAD 20 (1996) 471.
[12] T.M. Korhonen, J.K. Kivilahti, J. Electron. Mater. 27 (1998) 149.
[13] H. Ohtani, M. Miyashita, K. Ishida, J. Jpn. Inst. Met. 63 (1999) 685.
[14] A. Dinsdale, CALPHAD 15 (1991) 317.
[15] Y.-M. Muggianu, M. Gambino, L.P. Bros, J. Chim. Phys. 72 (1975) 85.
[16] B. Sundman, B. Jansson, J.O. Andersson, CALPHAD 9 (1985) 153.